Cancer Letters xxx (2018) xxx-xxx

Contents lists available at ScienceDirect

Cancer Letters

journal homepage: www.elsevier.com

Original Articles

Sulforaphane-N-Acetyl-Cysteine inhibited autophagy leading to apoptosis via Hsp70-mediated microtubule disruption

Yabin Hu[a, b], Yan Zhou[a, b], Gaoxiang Yang[a, b], Yalin Wang[a, b], Zhongnan Zheng[a, b], Juntao Li[a, b], Yuting Yan[a, b], Wei Wu[a, b, c, *]

[a] Department of Biochemistry and Molecular Biology, School of Basic Medical Sciences, China
[b] Beijing Key Laboratory of Tumor Invasion and Metastasis Research, Institute of Cancer Research, China
[c] Institute of Brain Tumor, Beijing Institute for Brain Disorders; Capital Medical University, No. 10, Xitoutiao, You An Men Wai Ave., Feng Tai District, Beijing, 100069, China

ARTICLE INFO

Keywords:
Sulforaphane metabolites
Autophagosome
Stathmin-1
α-tubulin
Lung cancer

ABSTRACT

Sulforaphane-N-acetyl-cysteine (SFN-NAC) is a potential drug to inhibit human non-small cell lung cancer (NSCLC), but the underlying mechanisms are elusive. Here, we uncovered that SFN-NAC induced apoptosis via flow cytometer assay and transmission electron microscopy. Further, SFN-NAC increased LC3 II/LC3 I and the number of LC3 punctas, but Western blot showed that SFN-NAC inhibited cell autophagy in response to a co-treatment of Bafilomycin A1 and SFN-NAC. Furthermore, immunofluorescence staining and Western blot showed that SFN-NAC triggered microtubule disruption causing apoptosis via downregulating α-tubulin and phosphorylated ERK1/2-mediated Stathmin-1. Besides, SFN-NAC upregulated Hsp70 via phosphorylating ERK1/2. Confocal microscopy and immunoprecipitation assay showed that SFN-NAC promoted the colocalization and interaction of Hsp70 and α-tubulin; knockdown of Hsp70 enhanced SFN-NAC-induced microtubule disruption, lowered LC3 II/LC3 I and promoted apoptosis. Interestingly, tissue microarray analysis showed that the increased expression of either α-tubulin or Hsp70 correlated to NSCLC malignant grading, indicating that microtubule and Hsp70 are two key targets for SFN-NAC. These results will give us a new insight into SFN-NAC-induced apoptosis so that we develop more efficient therapeutics to treat NSCLC.

1. Introduction

Those commonly used drugs for non-small cell lung cancer (NSCLC) might have side-effects and poor prognosis, thus it is necessary to develop low-toxicity and high-efficiency chemotherapeutics. Vegetable-derived sulforaphane (SFN) inhibited tumor progression in many cancers. However, due to a short half-life in circulation, higher working dose, unclear toxicity and drug resistance, SFN has not been used clinically yet. However, SFN might be metabolized in blood to produce sulforaphane-N-acetyl-cysteine (SFN-NAC) and sulforaphane-cysteine (SFN-Cys) [1]. SFN-NAC is the most abundant SFN metabolite in tissues and urine, and discharged completely from the animal body within 72h [2,3]. Although multiple mechanisms were found involving in SFN-induced apoptosis in a variety of cancers [4,5], whether SFN-NAC induced apoptosis in NSCLC remains unclear. Investigation of mechanisms which SFN-NAC might induce apoptosis will help us find novel molecular targets and establish efficient chemotherapies.

Recently, we reported that both SFN-NAC and SFN-Cys induced apoptosis via phosphorylated ERK1/2-mediated microtubule disruption in human prostate cancer cells [6]. As a main component of microtubule, α-tubulin plays an important role in cell motility, mitosis, intracellular trafficking, cytoskeleton remodeling and cell cycle [7]. Highly expressed α-tubulin was detected in tumor, thus α-tubulin was regarded as a biomarker for cancer grading and prognosis [8]. Microtubule disruption might result from microtubule depolymerization which was regulated by a balance of dynamics between the expressions of microtubule-stabilizing proteins and microtubule-destabilizing proteins. Similar to α-tubulin, microtubule destabilizing protein Stathmin-1 is a potential anti-cancer target. Highly expressed Stathmin-1 in many human cancers was thought to be correlated to tumor grading of malignancy and poor prognosis [9,10], while low expression of Stathmin-1 promoted the excessive stability of microtubule though lowering depoly-

* Corresponding author. Department of Biochemistry and Molecular Biology, School of Basic Medical Sciences, China.
Email address: weiwu207@ccmu.edu.cn (W. Wu)

https://doi.org/10.1016/j.canlet.2018.05.035
Received 13 February 2018; Received in revised form 23 May 2018; Accepted 23 May 2018
Available online xxx
0304-3835/

merization leading to apoptosis [11]. Besides, Stathmin-1 overexpression increased radioresistance via inducing autophagy in NSCLC cells [12]. SFN might regulate macroautophagy (abbreviated as autophagy) via phosphorylated ERK1/2; inhibition of ERK1/2 activation via U0126 prevented SFN-induced LC3 II elevation [13]. Interestingly, inhibition of autophagy via Cadmium was associated with microtubule disruption in nerve cells [14]. These findings pushed us to investigate whether SFN-NAC triggered apoptosis via regulating autophagy.

Studies showed that SFN regulated autophagy in pancreatic cancer cells [15], some molecular chaperones might modulate autophagy. SFN activated heat shock response and increased proteasome activity through upregulation of Hsp27, and Hsp27 might regulate cytoskeleton activity and maintain the conformational structure and stability of the interacting proteins [16,17]. Hsp70 was highly expressed in malignant cancer cells and involved in oncogenesis and chemotherapy resistance [18,19]. Further, Hsp70 regulated autophagy during cell growth and differentiation, and acetylated Hsp70 inhibited caspase-dependent apoptosis and autophagic cell death in cancer cells [20]. Furthermore, overexpressed Hsp70 prevented cell death triggered by chemical drugs and played a central role in stress-induced cell death by maintaining protein homeostasis [21,22]. Knockdown of Hsp70 via siRNA increased cell sensitivity to drugs [23]. In addition, Hsp70 helped the folding of newly synthesized polypeptides, the assembly of multiple protein complexes. Therefore, Hsp70 might interact with α-tubulin to regulate cell homeostasis. Since autophagy is a way to recycle and eliminate proteins, such as mitochondria and microtubule proteins via autophagolysosomes, SFN metabolites might regulate autophagy via Hsp70 to repair or clear up damaged microtubule proteins. Numerous studies showed the opposite results that inhibition of autophagy enhanced or lowered apoptosis in a number of cancer cells [24–28]. Hence we have to know the underlying mechanisms that SFN-NAC regulates autophagy and apoptosis.

In a word, the characterization of the mechanisms that SFN-NAC inhibits cancer will help us design a potential anti-cancer chemotherapy to treat NSCLC.

2. Materials and methods

2.1. Antibodies and reagents

Specific antibodies against pERK1/2, total ERK1/2, LC3, cleaved-caspase3 (Cell Signaling Technology, USA), Stathmin-1, α-tubulin (Abcam, UK), Hsp70 (Abclonal, China) were purchased. D, L-Sulforaphane-N-acetyl-cysteine (Santa Cruz Biotech, USA), pERK1/2 inhibitor PD98059 (Cell Signaling Technology, USA), autophagy inhibitor 3-Methyladenine (3-MA, Sigma, USA) and Bafilomycin A1 (Sellek, USA) were purchased.

2.2. Cell culture and transfection

Human NSCLC A549, SK-1, H1915 cells, normal bronchial epithelial 16HBE and BEAS-2B cells (Cell Resource Center, Peking Union Medical College) were cultured in DMEM/F12, RPMI-1640 medium or DMEM with 10% fetal bovine serum (Hyclone, USA). All cells were cultured in a humidified incubator in 5% CO_2 at 37 °C.

To knock down Hsp70 mRNA, negative control siRNA (NC siRNA) (5′-TTCTCCGAACGTGTCACGT-3′) and Hsp70 siRNA (5′-CGACGGAGACAAGCCCAAG-3′) were designed [29]. Cells were plated in 6-well plates (diameter, 35mm) at a density of 1×10^6/well and cultured for 24 h. Then the cells were transfected with the Hsp70 siRNA or NC siRNA (30 pmol/well) by Lipofectamine™ RNAiMAX (Invitrogen, USA) when cells reach approximately 80% confluency.

2.3. Morphology assay

Cells were seeded at a density of 1×10^5 cells/well in 6-well plates and incubated overnight. For treatment with SFN-NAC, fresh medium-containing 10% fetal bovine serum was added, and then cells were treated with different concentrations of SFN-NAC (0, 10, 20, 30, 40 and 50 μM) for 24 h. The morphological images of the cells were observed by phase contrast microscope at ×100 magnification (Leica, Germany) and photographed.

2.4. Cell viability assay

Cells were seeded at a density of 1×10^4 cells/well in 96-well plates and incubated overnight. Then cells were treated with different concentrations of SFN-NAC (0, 10, 20, 30, 40 and 50 μM) for 24 h. The method is given in Promega MTS instruction (Promega, USA).

2.5. Apoptosis assay

Cell apoptosis was measured via Annexin V-FITC apoptosis assay kit (GenStar, China). After treatment with SFN-NAC, the cells were harvested and washed twice with ice-cold phosphate-buffered saline (PBS), and the cells were resuspended to a concentration of 1×10^6 cells/mL by binding buffer. Then 5 μL Annexin V-FITC and 10 μL PI were added to 100 μL cell suspension, and the reaction was incubated for 5 min at room temperature in the dark. Apoptotic cells were detected via a flow cytometer.

2.6. Soluble and insoluble protein

The treated cells were washed with ice-cold PBS and lysed on ice by Nondenaturing Lysis Buffer (APPLYGEN, China) supplemented with protease inhibitors cocktail (Roch, Switzerland). The cell lysates were centrifuged at 12,000 rpm for 15 min at 4 °C. The supernatant was defined as the soluble protein and the pellet which was defined as the insoluble protein, was washed twice with ice-cold PBS and dissolved in 95 °C 2% SDS for 30 min.

2.7. Western blot

Cells were lysed by RIPA buffer (APPLYGEN, China) supplemented with protease inhibitors cocktail. Whole-cell lysates were quantified by the BCA Protein Assay Kit (APPLYGEN, China). Equal quantities of protein (30 μg) from each sample were separated by 10% or 15% SDS-PAGE; the whole procedures will be done by the protocol we published [30].

2.8. Coimmunoprecipitation

The treated cells were washed with ice-cold PBS, then lysed on ice via Nondenaturing Lysis Buffer supplemented with protease inhibitors cocktail. The monoclonal anti-α-tubulin or anti-Hsp70 were added to the protein lysates, incubated overnight at 4 °C. The complexes were pulled down with protein A/G agarose for 3 h and the proteins were isolated by centrifuging and boiling for 5 min. Western blot was used to recognize the conjugated proteins.

2.9. Immunofluorescence and confocal microscopy

Cells were treated with 30 μM SFN-NAC for 24 h and fixed with 1% paraformaldehyde for 15 min and permeabilized with methanol -20 for 10 min at room temperature. After blocking, the cells were incubated

with the corresponding primary antibodies and further the fluorescence-labeled secondary antibody. The cells were stained with DAPI (Zsgb-bio, China). Fluorescence images were collected under a laser scanning confocal microscope (LSCM) (Olympus FV1000, Japan).

2.10. Transmission electron microscopy (TEM)

Cells were harvested and fixed with 3% glutaraldehyde at 4 °C for 2 h. After washing with PBS for three times, the samples were fixed in 1% osmium tetroxide for 1 h. Then samples were dehydrated through a graded ethanol series and embedded in a 1:1 mixture of acetone and Epon812 resin for 30 min. The samples were then infiltrated 2 h in Epon812. Ultrathin sections were cut with a knife and placed on 200-mesh copper grids and stained with Uranium acetate for 30 min and Lead nitrate for 20 min. The sections were then examined and photographed with a transmission electron microscope (JEM-1400Plus, Japan).

2.11. Immunohistochemistry

Human lung adenocarcinoma and lung squamous carcinoma tissue arrays containing 150 dotted tumor and adjacent tissues from 75 patients with different pathologic grading grades were purchased from Shanghai Biochip (Shanghai, China). The immunohistochemistry stain was done with human specific anti-Hsp70 or anti-α-tubulin combined with the UltraSensitive™ S-P detection kit (Maixin, Fuzhou, China). The protocol derived from the recently published paper [6].

2.12. Statistical analysis

All data were expressed as mean ± standard deviation (SD) from 3 independent experiments. Paired data were evaluated by Mann Whitney test. $P \leq 0.05$ was considered statistically significant. Multiple independent data were evaluated by Kruskal-Wallis test. $P \leq 0.01$ was considered statistically significant. The statistical analyses were done by SPSS version 19.0.

3. Results

3.1. SFN-NAC inhibited cell proliferation and induced apoptosis in NSCLC cells

Cells were treated with SFN-NAC at the indicated concentrations for 24 h. Results showed that SFN-NAC induced morphological alterations in both A549 and SK-1 cells (Fig. 1A). SFN-NAC-treated cells got shrunk, round and more transparent with short processes after treated with 30 μM SFN-NAC. In addition, cell viability was inhibited by SFN-NAC in a concentration-dependent manner. In contrast, human normal

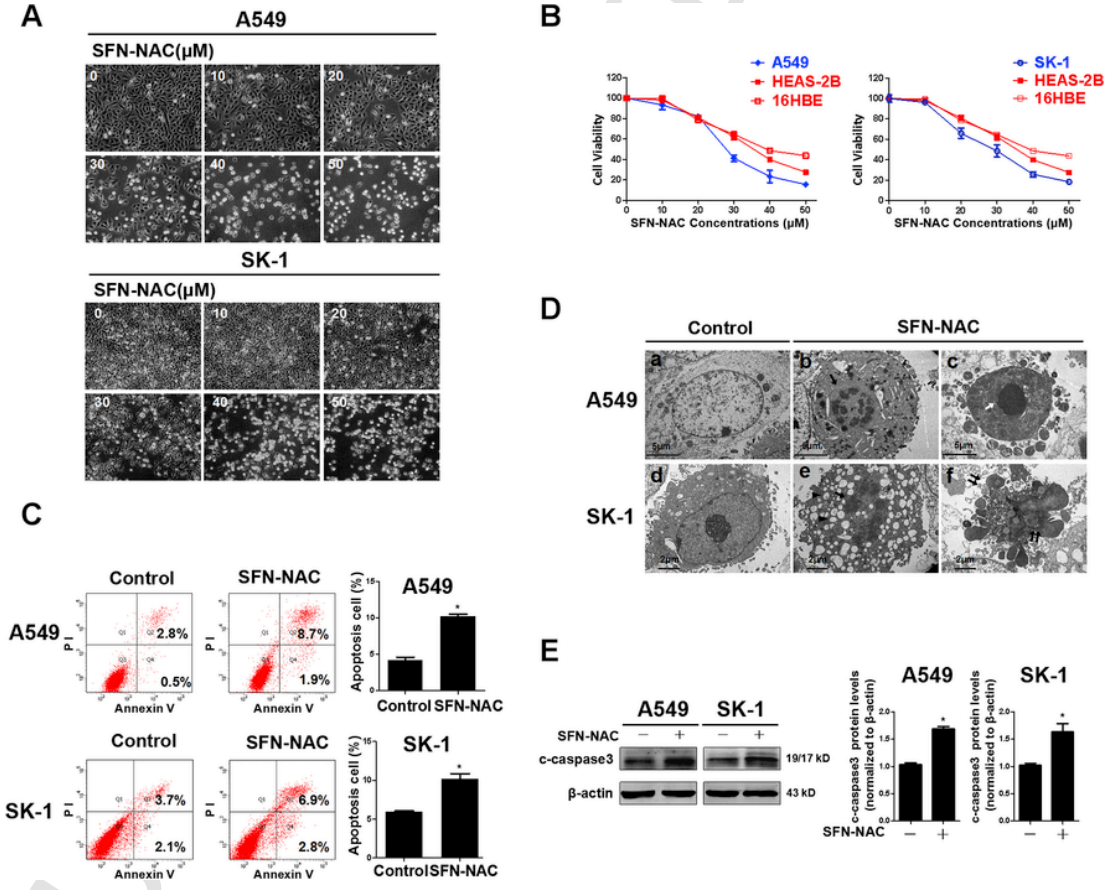

Fig. 1. SFN-NAC induced cell morphological alterations, inhibited cell proliferation and caused apoptosis. **A:** Both A549 and SK-1 cells were treated with SFN-NAC at the indicated concentrations for 24 h. Then, cell morphological images were observed by Leica DMIRB microscope (at × 100 magnification). **B:** A549, SK-1, BEAS-2B and 16HBE cells were treated with SFN-NAC at the indicated concentrations for 24 h. Then, cell viability was determined by Cell Proliferation Assay Kit and presented as the percentages versus the control. **C:** Both A549 and SK-1 cells were treated with 30 μM SFN-NAC for 24 h, then the cells were harvested and the percentage of cell apoptosis was analyzed by flow cytometer via Annexin V-FITC/PI Apoptosis Detection Kit. **D:** After induction with 30 μM SFN-NAC, both A549 and SK-1 cells were harvested and fixed, the cells pellets were cut into thin slices and stained with Uranium acetate and Lead nitrate, and finally were viewed with a TEM. Black arrows indicate nucleic fragmentation, white arrows indicate nucleic condensation, black arrowheads indicate sporadic vacuoles and double black arrows indicate apoptotic bodies. Scale bars: (a–c: 5 μm), (d–g: 2 μm). **E:** Western blot analysis of cleaved-caspase3 expression in A549 and SK-1 cells treated with SFN-NAC (c-caspase3: cleaved-caspase3). *, $P \leq 0.05$, SFN-NAC only cells versus the control cells. Data were shown as means ± SD ($n = 3$).

bronchial epithelial BEAS-2B and 16HBE cells were significantly less sensitive to SFN-NAC (Fig. 1B). Cell flow cytometer assay showed that SFN-NAC increased apoptosis in both cancer cell lines (Fig. 1C). TEM observation showed that SFN-NAC-treated cells displayed apoptotic phenotypes, such as nuclear fragmentation, nucleic condensation, sporadic vacuoles and apoptotic bodies (Fig. 1D). More, Western blot showed that SFN-NAC elevated the level of cleaved-caspase3 in both cancer cell lines (Fig. 1E). The concentration of 30 μM, as IC50, was set as a concentration to investigate the signaling, the treatment time of 24 h was the optimal time to consistently activate ERK1/2.

3.2. The upregulation of Hsp70 resulted from the phosphorylated ERK1/2

Cells were treated with SFN-NAC at the indicated concentrations and times. These results showed that SFN-NAC upregulated the expression of pERK1/2 in either a time-dependent manner (Fig. 2A) or a concentration-dependent manner (Fig. 2B). More, SFN-NAC also elevated the level of Hsp70 significantly (Fig. 2C and D). To determine the relationship between ERK1/2 phosphorylation and Hsp70 upregulation, a specific inhibitor of phosphorylated ERK1/2, PD98059 (25 μM) was applied. PD98059 reversed the upregulation of phosphorylated ERK1/2 (Fig. 2E), indicating that SFN-NAC-induced pERK1/2 upregulation resulted in the upregulation of Hsp70.

3.3. High expression of Hsp70 was detected in NSCLC tissues

The expression of Hsp70 was tested via immunohistochemistry (IHC) staining on tissue arrays of human lung adenocarcinoma and lung squamous carcinoma samples. Hsp70 intensity in tumor tissues was raised as the pathological grading increased, but the density in the adjacent tissues was significantly lower (Fig. 2F). In addition, the H-

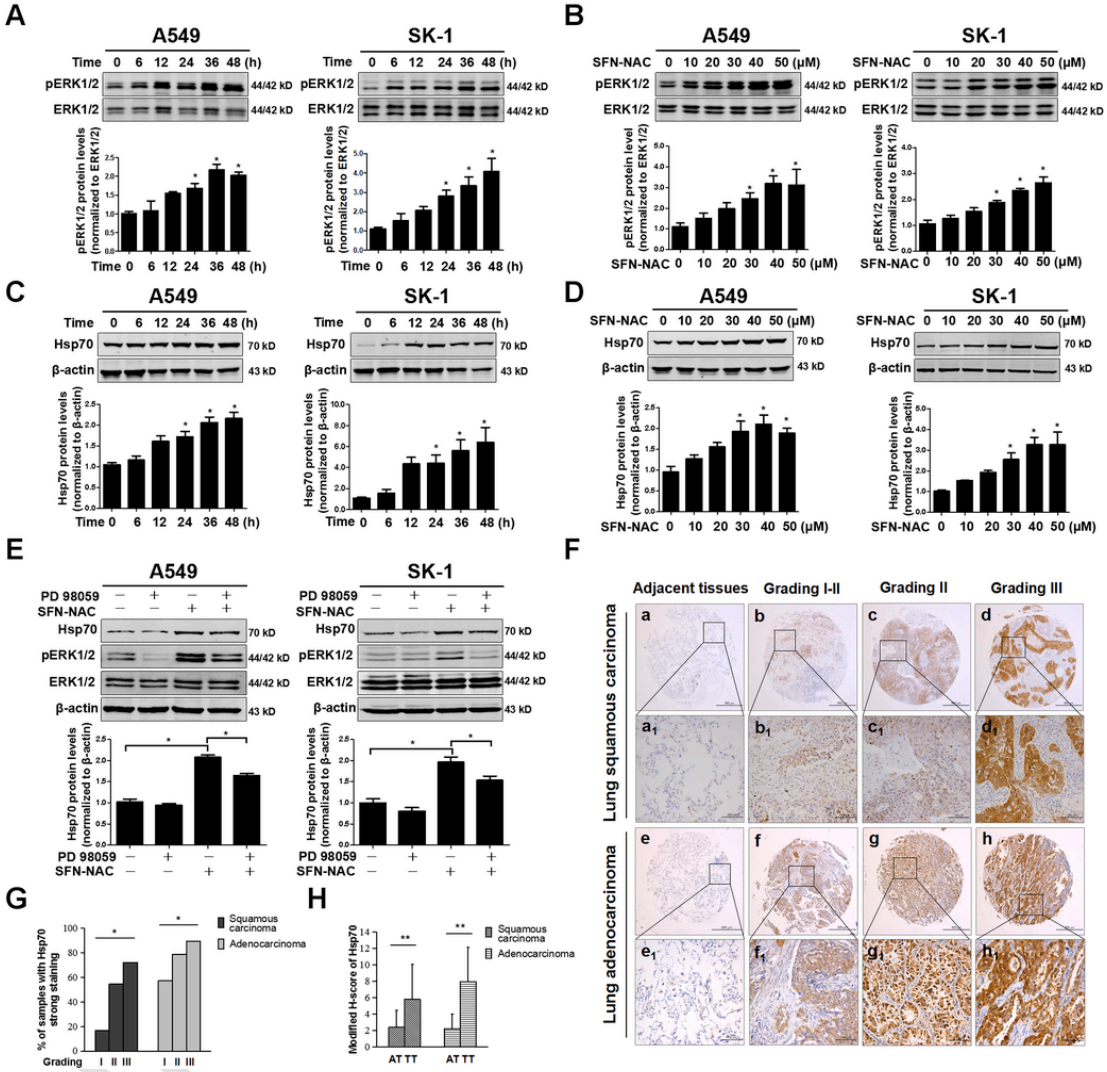

Fig. 2. SFN-NAC upregulated Hsp70 via phosphorylated ERK1/2 and higher Hsp70 staining linked to NSCLC malignant grading. A-B: Western blot analysis of pERK1/2 expression in A549 and SK-1 cells treated with SFN-NAC at the indicated time phases (**A**) or at the indicated concentrations (**B**). **C-D:** Western blot analysis of Hsp70 expression in both A549 and SK-1 cells treated with SFN-NAC at the indicated time phases (**C**) or at the indicated concentrations (**D**). **E:** Both A549 and SK-1 cells were pretreated with PD98059 (25 μM) for 30 min, then treated with SFN-NAC (30 μM) for 24 h. The expression of Hsp70 and phosphorylated ERK1/2 were analyzed by Western blot. **F:** Hsp70 expression was evaluated in the arrayed tissues with pathological grades of lung adenocarcinoma and lung squamous carcinoma. IHC of Hsp70 in adjacent (a, a_1 and e, e_1) and cancer tissues with three malignant grades (b-d, b_1-d_1 and f-h, f_1-h_1) of lung adenocarcinoma and lung squamous carcinoma were used. Upper panel: magnification × 50. Scale bars: 500 μm; lower panel: magnification × 200. Scale bars: 100 μm. **G:** Percentages of samples with strong Hsp70 staining in adjacent tissues and tumor tissues which were divided into three malignant grades. **H:** The comparison of H scores for Hsp70 expression between adjacent and tumor tissues were done in lung adenocarcinoma and lung squamous carcinoma (AT: adjacent tissues; TT: tumor tissues). Data were shown as means ± SD ($n \geq 3$). *, $P \leq 0.01$; **, $P \leq 0.001$.

scores of tumor tissues by IHC staining corresponding to Hsp70 were higher than those of adjacent tissues (Fig. 2G).

The correlation of Hsp70 expression to pathological grading of NSCLC was analyzed by calculating the H-score (Table 1). The results indicated that the level of Hsp70 expression seemed to be positively correlated with the pathological grading of the lung adenocarcinoma or squamous carcinoma (Fig. 2H). No correlation was detected between highly expressed Hsp70 and other clinical parameters.

These findings suggested that Hsp70 overexpression may be required for lung tumorigenesis or for the maintenance of its malignant phenotypes.

3.4. SFN-NAC downregulated α-tubulin resulting in microtubule disruption

Herein we found SFN-NAC dramatically downregulated the expression of α-tubulin and in a time and concentration-dependent manner (Fig. 3A and B). In addition, when these cells were treated with SFN-NAC for 24 h, we observed a decrease in the amount of α-tubulin in both soluble and insoluble fractions compared with the untreated control cells (Fig. 3C). These indicated that SFN-NAC depolymerized microtubule. Further, the results of immunofluorescence also showed that SFN-NAC induced microtubule disorganization and aggregation in both A549 and SK-1 cells (Fig. 3D). These implied that SFN-NAC disrupted microtubules in both cell lines. Similar to the results of Hsp70 test in tissue arrays of human lung adenocarcinoma and lung squamous carcinoma samples, α-tubulin intensity was raised as the pathological grading increased, while those in the adjacent tissues were not significantly stained (Fig. 3E). In addition, the H-scores of tumor tissues by IHC staining with α-tubulin were higher than those of adjacent tissues (Fig. 3F).

The correlation of α-tubulin expression to pathological grading of NSCLC was also calculated by H-score (Table 2). The results indicated that the level of α-tubulin expression seemed to be positively correlated with the pathological grading of the lung adenocarcinoma and squamous carcinoma samples (Fig. 3G). No correlation was detected between highly expressed α-tubulin and gender, age and clinical staging.

These findings suggested that α-tubulin might serve as a biomarker for the deterioration of lung tumors.

3.5. SFN-NAC downregulated the expression of Stathmin-1 and promoted the interaction between Hsp70 and α-tubulin

Considering the undetectable expression of Stathmin-1 in SK-1 cells, we used a human lung squamous carcinoma cell line H1915 to be a substitute. Here, SFN-NAC downregulated the expression of Stathmin-1 (Fig. 4A and B) and this effect was reversed by PD98059 (Fig. 4C). However, SFN-NAC-induced downregulation of Stathmin-1 is significantly enhanced by Hsp70 silencing (Fig. 4D). These data indicated that pERK1/2 contributed to downregulation of Stathmin-1, while Hsp70 inhibited SFN-NAC-induced downregulation of Stathmin-1. Further, knockdown of Hsp70 resulted in a lower expression of α-tubulin (Fig. 4E). Furthermore, we also found that SFN-NAC enhanced the interaction between Hsp70 and α-tubulin (Fig. 4F). The results via immunofluorescence and confocal microscopy also showed that SFN-NAC promoted the colocalization of Hsp70 and α-tubulin (Fig. 4G). These data indicated that Hsp70 resisted the SFN-NAC-induced downregulation of α-tubulin and phosphorylated ERK1/2-mediated Stathimin-1, suggesting that Hsp70 is a microtubule protector.

3.6. SFN-NAC inhibited autophagy leading to apoptosis

Herein we observed autophagic features, such as autophagosome and autophagolysosome in SFN-NAC-treated cells (Fig. 5A). Moreover, SFN-NAC increased the number of LC3 punctas (Fig. 5B) and induced a decrease in LC3 I and an increase in LC3 II (Fig. 5C and D). To determine how SFN-NAC regulates autophagy, Bafilomycin A1 (100nM) was used. Results showed that SFN-NAC did not change LC3 II level after combined with Bafilomycin A1 (Fig. 5E). These results indicated that SFN-NAC inhibited autophagy. Another specific inhibitor of autophagy 3-MA (2.5mM) was used in the SFN-NAC treated cells. Results showed that inhibition of autophagy increased SFN-NAC-induced apoptosis (Fig. 5F), indicating that autophagy protected NSCLC cells from SFN-NAC-induced apoptosis.

3.7. Hsp70 repressed apoptosis via increasing LC3 II/LC3 I

To determine how Hsp70 links to SFN-NAC-induced microtubule disruption, autophagy inhibition and apoptosis, Hsp70 siRNA was used to knock down its expression. Results showed that knockdown of

Table 1
Correlation of Hsp70 expression to clinicopathological characteristics of lung cancer patients.

Variables	Lung squamous carcinoma				Variables	Lung adenocarcinoma			
	All patients	Low	High	*p* value		All patients	Low	High	*p* value
Gender				0.463	Gender				0.259
Male	71	31	40		Male	39	11	28	
Female	4	1	3		Female	35	6	29	
Age (years)				0.365	Age (years)				0.204
< =60	35	13	22		< =60	34	10	24	
>60	40	19	21		>60	41	7	34	
Differentiation				0.016[a]	Differentiation				0.032[a]
I	6	5	1		I	14	6	8	
II	44	20	24		II	42	9	33	
III	25	7	18		III	19	2	17	
Staging				0.947	Staging				0.807
IA	9	6	3		IA	14	2	12	
IB	14	4	10		IB	23	7	16	
IIA	13	4	9		IIA	14	3	11	
IIB	10	5	5		IIB	4	0	4	
IIIA	22	10	12		IIIA	11	4	7	
IIIB	2	1	1		IIIB	3	0	3	
IV	4	2	3		IV	4	0	4	

Low (Score 0–4), High (Score 5–12).

[a] $p < 0.05$ was defined as statistically significant.

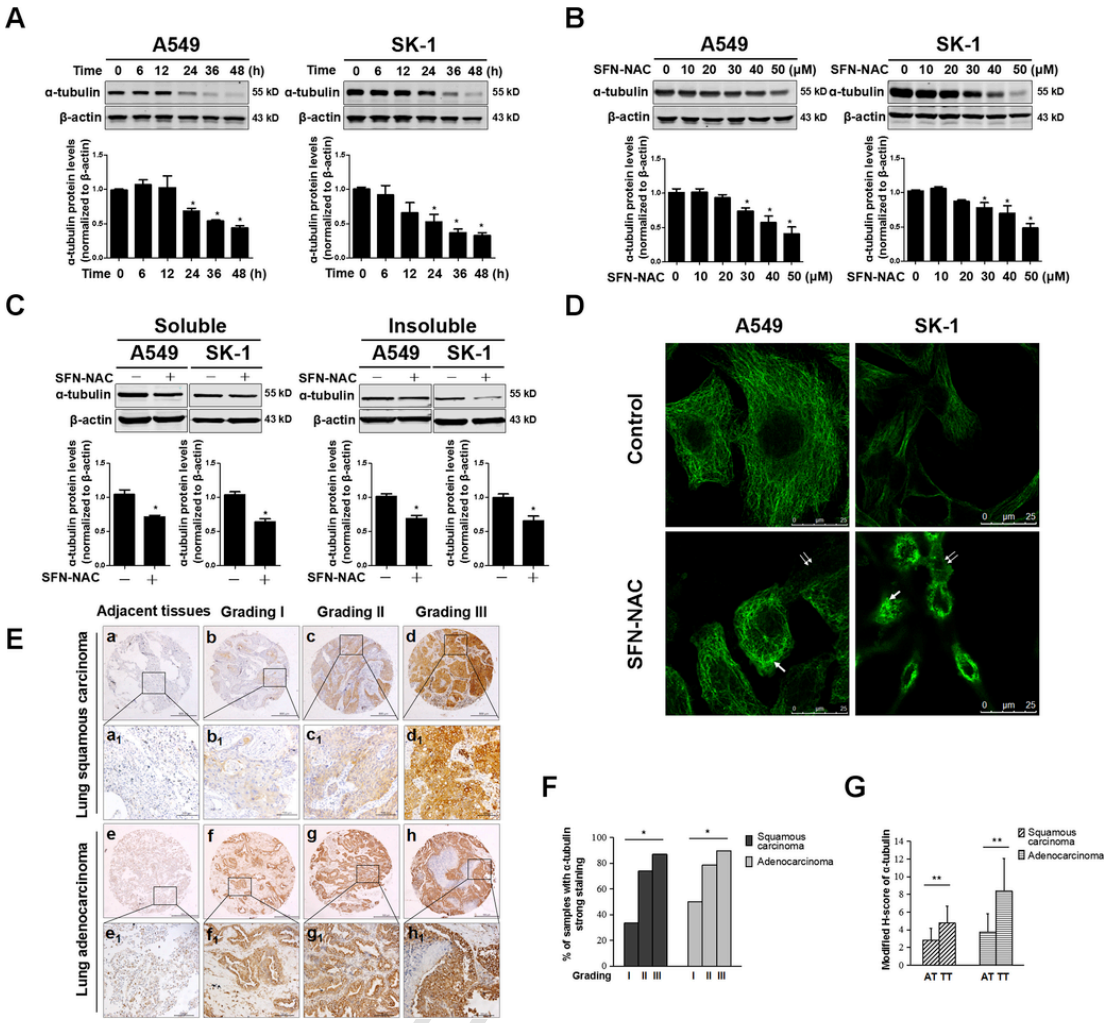

Fig. 3. SFN-NAC lowered the expression of α-tubulin causing microtubule disruption and higher α-tubulin staining linked to NSCLC malignant grading. A-B: Western blot analysis of α-tubulin expression in both A549 and SK-1 cells treated with SFN-NAC at the indicated time phases (**A**) or at the indicated concentrations (**B**). **C:** Western blot analysis of the expression of soluble and insoluble α-tubulin in both A549 and SK-1 cells. **D:** The structure of microtubule was observed under an LSCM. Arrows indicate microtubule aggregation and double arrows indicate microtubule disorganization. Scale bar: 25 μm. **E:** α-tubulin expression was evaluated in the arrayed tissues with pathological grades of lung squamous carcinoma. IHC of α-tubulin in adjacent (a) and cancer tissues with three malignant grades (b-f) of lung squamous carcinoma were used. Magnification × 200, Scale bars: 100 μm. **F:** Percentages of samples with strong α-tubulin staining in adjacent tissues and tumor tissues which were divided into three malignant grades. G: The comparison of H scores for α-tubulin expression between adjacent and tumor tissues were done in lung squamous carcinoma (AT: adjacent tissues; TT: tumor tissues). Data were shown as means ± SD ($n \geq 3$). *, $P \leq 0.01$; **, $P \leq 0.001$.

Hsp70 resulted in a significantly increased apoptosis (Fig. 6A), and a significantly increased microtubule disruption in response to SFN-NAC (Fig. 6B). In particular, knockdown of Hsp70 significantly decreased LC3 II/LC3 I in response to SFN-NAC (Fig. 6C). These data indicated that Hsp70 lowered SFN-NAC-induced apoptosis via increasing LC3 II/LC3 I.

Collectively, we demonstrated that SFN-NAC-induced microtubule disruption contributed to autophagic inhibition and apoptosis. Cell apoptosis was regulated via Hsp70-mediated autophagy which is a feedback of SFN-NAC treated NSCLC cells (Fig. 6D).

4. Discussion

We previously unveiled some novel mechanisms regarding SFN metabolites-induced tumor suppression in a couple of cancers [31,32]. Here we further discovered that SFN-NAC induced ERK1/2 phosphorylation and upregulated Hsp70 leading to Hsp70-mediated microtubule disruption, autophagy inhibition and apoptosis.

SFN can cause apoptosis and inhibit invasion by binding to its target proteins. Macrophage migration inhibitory factor (MIF) was demonstrated as a SFN-binding target, SFN covalently binding to MIF may constitute a novel anti-cancer mechanism via inducing apoptosis [33]. However, more studies showed that α-tubulin was the major binding target for SFN [34,35]. SFN was demonstrated to bind to α-tubulin to degrade α-tubulin causing apoptosis [36]. These results are consistent with the present findings. More studies in our and the other laboratories showed that SFN and its metabolites activated caspase3 resulting in α-tubulin degradation, aggregation and apoptotic phenotypes [30]. Degradation of α-tubulin might lead to cytoskeletal disassembly, cell morphological alteration, such as the formation and release of apoptotic bodies or vacuoles [37]. Therefore, SFN metabolites might induce α-tubulin/associated protein misfolding, degradation and aggregation leading to disequilibrium of microtubule dynamics. Studies showed that SFN treatment caused microtubule depolymerization and apoptosis in human lung cancer A549 cells [34]. Hence, the disruption of microtubule and the dysfunction of the associated proteins might be a key to cause cell death. Through tissue microarray assay, we demonstrated that increasing expression of α-tubulin contributed to cancer progression and grading of malignancy. Apparently, α-tubulin/associated proteins were the key therapeutic targets of SFN metabolites.

Table 2
Correlation of α-tubulin expression to clinicopathological characteristics of lung cancer patients.

Variables	Lung squamous carcinoma				Variables	Lung adenocarcinoma			
	All patients	Low	High	*P* value		All patients	Low	High	*P* value
Gender				0.178	Gender				0.822
Male	67	16	51		Male	39	10	29	
Female	4	2	2		Female	35	8	27	
Age (years)				1	Age (years)				0.532
< =60	33	7	26		< =60	34	7	27	
>60	38	11	27		>60	41	11	30	
Differentiation				0.025[a]	Differentiation				0.028[a]
I	6	4	2		I	14	7	7	
II	42	11	31		II	42	9	33	
III	23	3	20		III	19	2	17	
Staging				0.178	Staging				0.16
IA	9	2	7		IA	14	3	11	
IB	12	0	12		IB	23	8	15	
IIA	13	6	7		IIA	14	1	13	
IIB	10	3	7		IIB	4	0	4	
IIIA	20	6	14		IIIA	11	5	6	
IIIB	2	0	2		IIIB	3	0	3	
IV	5	1	4		IV	4	0	4	

Low (Score 0–4), High (Score 5–12).
[a] $p < 0.05$ was defined as statistically significant.

Studies showed that ERK1/2-mediated Stathmin-1 phosphorylation plays an important role in the microtubule reorganization [38]. More, p38 activation promoted microtubule disruption by phosphorylating the microtubule-associated protein 4 (MAP4) and dephosphorylating Stathmin-1 [39]. Hereby we found that SFN-NAC downregulated Stathmin-1 via pERK1/2 and the upregulated Hsp70 prevented the downregulation of Stathmin-1. These results showed that Stathmin-1 either sequestered tubulin dimers or stimulated microtubule catastrophes leading to promotion of microtubule disassembly. Therefore, these results that SFN-NAC downregulated Stathmin-1 might contribute to microtubule disassembly. Minor change of microtubule dynamics is able to affect the cell cycle leading to apoptosis, the concentration of free tubulin heterodimers is also crucial for microtubule assembly compared with microtubule-associated protein phosphorylation [40]. We determined that SFN-NAC induced degradation of soluble or insoluble α-tubulin, which might influence microtubule treadmilling and shortening leading to microtubule disruption. Imbalance of microtubule dynamics might cause cell apoptosis and impede autophagy by inhibiting autophagosome-lysosome fusion [41]. Coincidentally, here we found that SFN-NAC increased LC3 II/LC3 I and the number of LC3 punctas, but we are not sure whether SFN-NAC inhibited autophagosome-lysosome fusion. Likewise, studies showed that SFN regulated autophagy was associated with upregulation and recruitment to autophagosomes of microtubule-associated protein 1 light chain 3 (LC3), which was proved to link autophagosome to lysosome [42,43]. Attenuation of LC3 via 3-MA accelerated apoptosis [44]. Therefore, autophagy might be a repressor of microtubule dysfunction via recycling degraded components of microtubules.

Hsp70 regulated autophagy and the dynamics of microtubule via interacting with microtubule associated proteins. In the present study, Hsp70 interacts with unfolded and aggregated proteins, such as degraded α-tubulin to repair damaged proteins, refold unfolded proteins and reduce microtubule protein aggregation. More, Hsp70 was reported to promote the stabilization of lysosome leading to autophagy and cancer cell survival [45], and inhibition of Hsp70 caused disruption of autophagy as it induced aberrant aggregation and oligomerization of the autophagic scaffold protein p62/SQSTM1 [46]. Additionally, knockdown of Stathmin-1 inhibited basal and rapamycin-induced autophagy [47]. Similarly, we also found knockdown of Hsp70 enhanced SFN-NAC-induced downregulation of Stathmin-1 and reduced autophagy in response to SFN-NAC. These results demonstrated that Hsp70-mediated autophagy might inhibit apoptosis resulting from microtubule disruption. Interestingly, inhibition of autophagy by 3-MA increased apoptosis, thus Hsp70 upregulation and Hsp70-mediated autophagy might be a protective response of cells to resist apoptosis. Hsp70 inhibited apoptosis and its high expression in tumors was associated with poor prognosis and higher resistance to anticancer treatment, which matched the present results in the tissue microarray assay [18,19]. Since Hsp70 represses apoptosis through inhibition of the both intrinsic and extrinsic apoptotic pathways and depletion of Hsp70 with siRNA promoted cell death and sensitized malignant cells to chemotherapy, we believed that Hsp70 might be a key target for cancer therapy [48,49].

Taken together, we uncovered a brand-new mechanism that SFN-NAC induced apoptosis via microtubule disruption. These results might help us evaluate the anti-cancer potential of SFN-NAC to establish an efficient anti-cancer chemotherapy.

Author contributions

W. W. conceived, designed and supervised the entire project. W. W., Y.B. H. and Y. Z. developed the methodology. Y. Z., G. X. Y. and Y. L. W. acquired the data. Y. Z, G. X. Y, Y. B. H. and Y. L. W. analyzed and interpreted the data (e.g., statistical analysis and computational analysis). W. W., Y. B. H. and Y. Z. wrote, revised the manuscript. Y. L. W., Z. N. Z., J. T. L., and Y. T. Y. provided administrative and technical support (i.e., organizing data and constructing databases).

Disclosure of potential conflicts of interest

No potential conflicts of interest were disclosed.

Conflicts of interest statement

No conflict of interest exits in the submission of this manuscript, and manuscript is approved by all authors for publication.

Acknowledgments

Thank the National Natural Science Foundation of China (grant no. 81272843 and 81601993) for supporting this study.

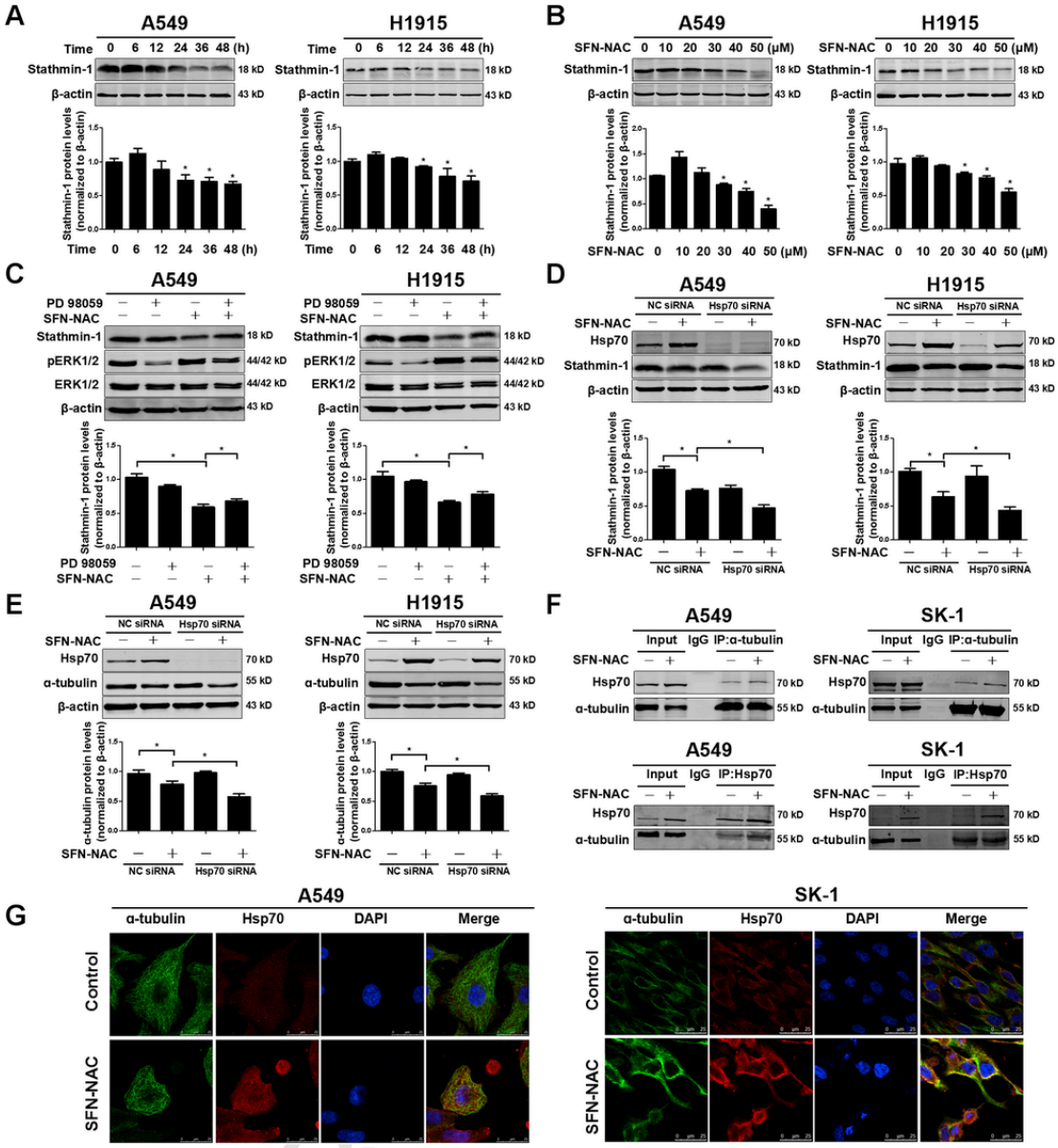

Fig. 4. SFN-NAC downregulated the expression of Stathmin-1 and promoted the interaction between α-tubulin and Hsp70. A-B: Western blot analysis of Stathmin-1 expression in both A549 and SK-1 cells treated with SFN-NAC at the indicated time phases (**A**) or at the indicated concentrations (**B**). **C:** Both A549 and SK-1 cells were pretreated with PD98059 (25 μM) for 30 min, then treated with SFN-NAC (30 μM) for 24 h. The expressions of Stathmin-1 and pERK1/2 were analyzed by Western blot. **D:** Both A549 and H1915 cells were transfected with NC siRNA or Hsp70 siRNA. After transfection for 48 h, the cells were treated with SFN-NAC for 24 h. Then the cells lysates were harvested and the expression of Hsp70 and Stathmin-1 was analyzed by Western blot. **E:** Western blot analysis of α-tubulin and Hsp70 expression in both A549 and SK-1 cells transfected with NC siRNA or Hsp70 siRNA. **F:** After induction with 30 μM SFN-NAC for 24 h, coimmunoprecipitation was employed to detect the interaction between α-tubulin and Hsp70 in both A549 and SK-1 cells. **G:** immunofluorescence and confocal microscopy were employed to observe the colocalization of α-tubulin and Hsp70 in both A549 and SK-1 cells. Scale bar: 25 μm. Data were shown as means ± SD ($n \geq 3$). *, $P \leq 0.01$.

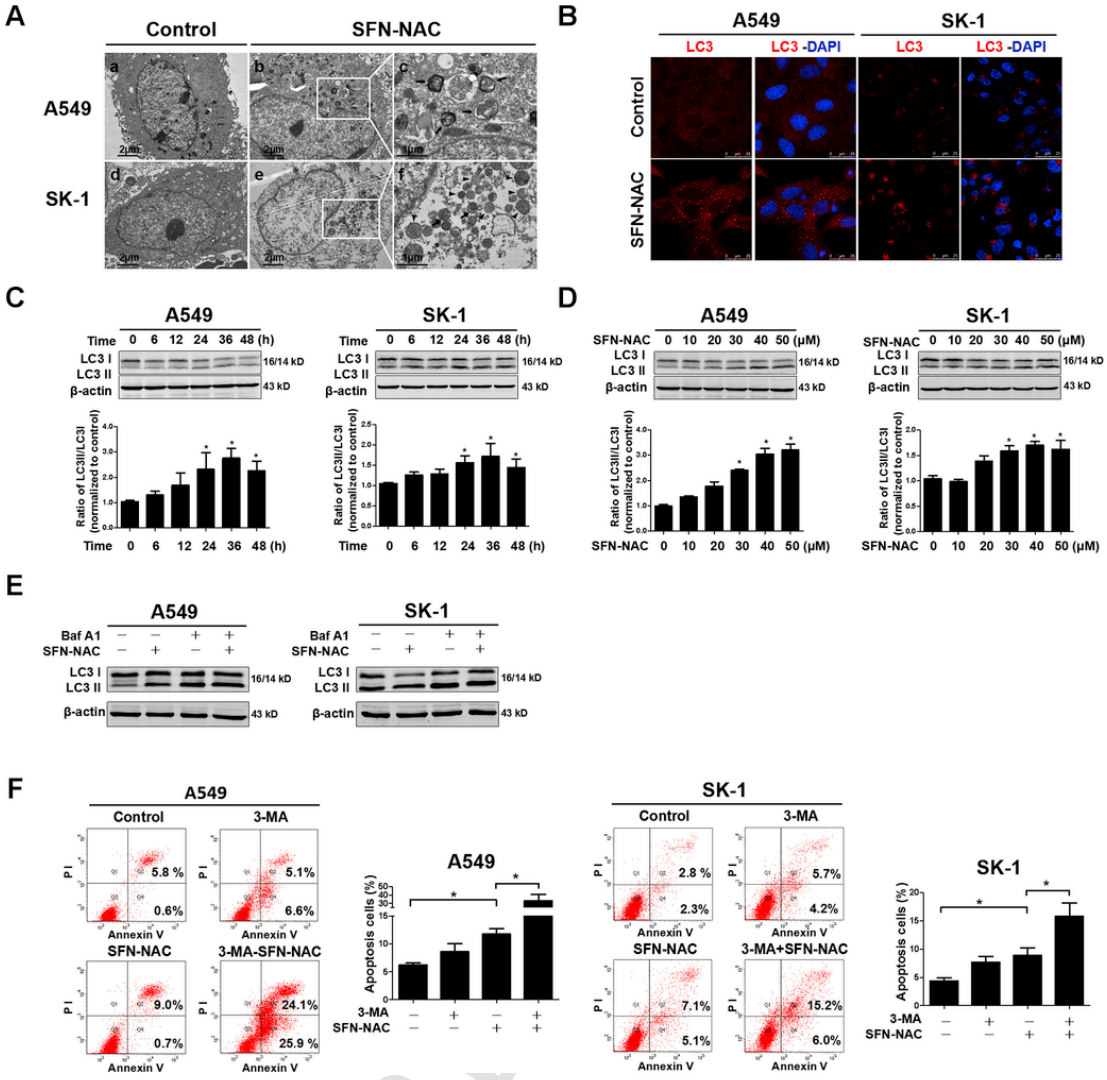

Fig. 5. SFN-NAC inhibited autophagy increasing apoptosis. **A:** Observation via TEM showed the autophagosome and autophagolysosome in both A549 and SK-1 cells treated with the SFN-NAC (30 μM). Arrows indicate autophagosome, arrowheads indicate autophagolysosome. Scale bar: (a-b, d–e: 2 μm), (c, f: 1 μm). **B:** The immunofluorescence and confocal microscopy data showed that the SFN-NAC increased LC3 punctas in both A549 and SK-1 cells, indicating the formation of autophagosome. Scale bar: 25 μm. **C-D:** Western blot analysis of LC3 I and LC3 II expression in A549 and SK-1 cells treated with SFN-NAC at the indicated time phases (**C**) or at the indicated concentrations (**D**). The relative ratio of LC3 II/LC3 I was calculated via the gray scale analysis. **E**: A549 and SK-1 cells co-treated with Baf A1 (100 nM) and SFN-NAC (30 μM) for 24 h, the expression of LC3 I and LC3 II was determined by Western blot. **F**: A549 cells and SK-1 cells were pretreated with 2.5 mM 3-MA, and then SFN-NAC was added into the cell medium after 2 h. After incubation for 24 h, the cells were harvested and the apoptosis cell number was determined by flow cytometer. (Baf A1: Bafilomycin A1) Data were shown as means ± SD (n ≥ 3). *, P ≤ 0.01.

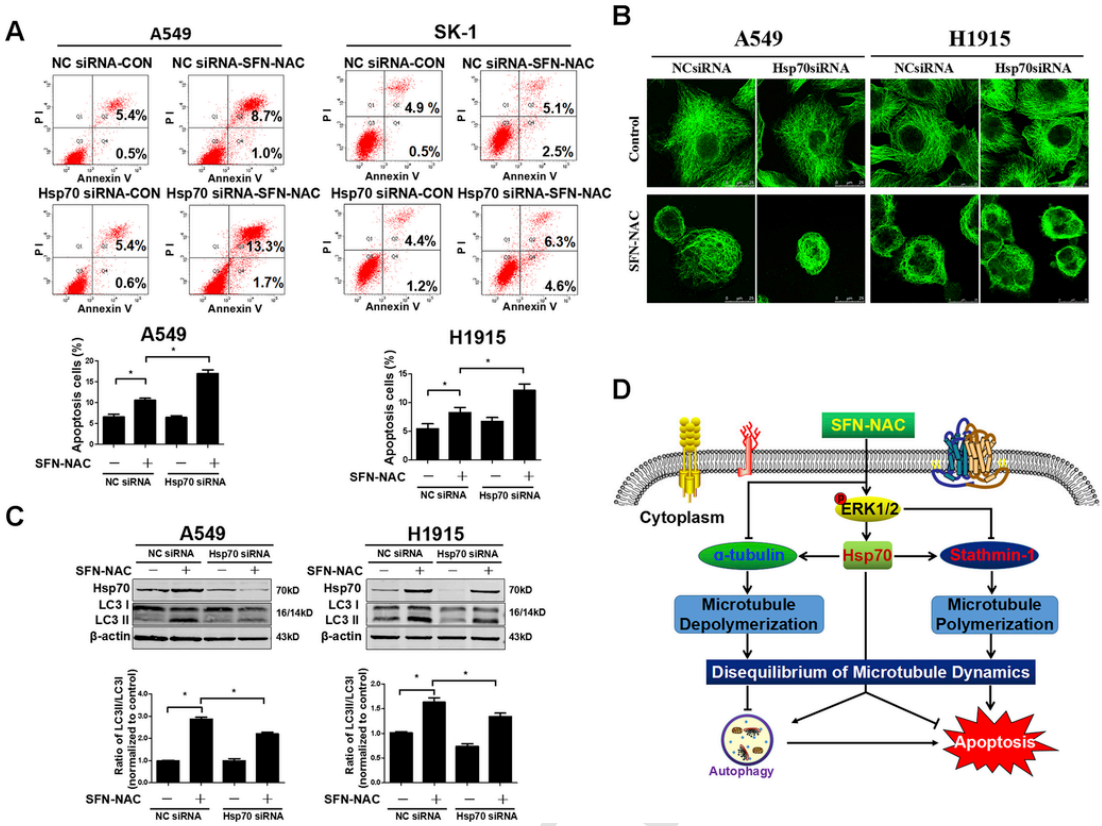

Fig. 6. Hsp70 played a central role in the autophagy-mediated apoptosis. A: Both A549 cells and H1915 cells were transfected with NC siRNA or Hsp70 siRNA, after transfection for 48 h, cells were treated with SFN-NAC (30 μM) for 24 h, the apoptosis cell number was determined by flow cytometer. **B:** Both A549 and H1915 cells were transfected with NC siRNA or Hsp70 siRNA. After transfection for 48 h, the cells were treated with SFN-NAC for 24 h. The structure of microtubule was observed under an LSCM. **C:** Both A549 and H1915 cells were transfected with NC siRNA or Hsp70 siRNA, and treated with SFN-NAC (30 μM) for 24 h, the expression of LC3 I and LC3 II was determined by Western blot. **D:** A possible schematic of the involved signal pathways that SFN-NAC induced disequilibrium of microtubule dynamic leading to apoptosis and autophagy inhibition in NSCLC cells. SFN-NAC downregulated the expression of α-tubulin and Stathmin-1 leading to a disrupted microtubule and ultimately induced apoptosis, and upregulated Hsp70 via increasing pERK1/2 promoted autophagic phenotype and inhibited apoptosis. Data were shown as means ± SD ($n \geq 3$). *, $P \leq 0.01$.

References

[1] A.T. Dinkova-Kostova, R.V. Kostov, Glucosinolates and isothiocyanates in health and disease, Trends Mol. Med. 18 (2012) 337–347.

[2] A.V. Gasper, A. Al-Janobi, J.A. Smith, J.R. Bacon, P. Fortun, C. Atherton, et al., Glutathione S-transferase M1 polymorphism and metabolism of sulforaphane from standard and high-glucosinolate broccoli, Am. J. Clin. Nutr. 82 (2005) 1283–1291.

[3] J.D. Clarke, A. Hsu, D.E. Williams, R.H. Dashwood, J.F. Stevens, M. Yamamoto, et al., Metabolism and tissue distribution of sulforaphane in Nrf2 knockout and wild-type mice, Pharm. Res. (N. Y.) 28 (2011) 3171–3179.

[4] S.L. Martin, R. Kala, T.O. Tollefsbol, Mechanisms for inhibition of colon cancer cells by sulforaphane through epigenetic modulation of microRNA-21 and human telomerase reverse transcriptase (hTERT) down-regulation, Curr. Cancer Drug Targets 18 (2017) 97–106.

[5] J.R. Devi, E.B. Thangam, Mechanisms of anticancer activity of sulforaphane from Brassica oleracea in HEp-2 human epithelial carcinoma cell line, Asian Pac. J. Cancer Prev. APJCP 13 (2012) 2095–2100.

[6] Y. Zhou, G. Yang, H. Tian, Y. Hu, S. Wu, Y. Geng, et al., Sulforaphane metabolites cause apoptosis via microtubule disruption in cancer, Endocr. Relat. Canc. 25 (2018) 255–268.

[7] M. Barisic, H. Maiato, The tubulin code: a Navigation system for chromosomes during mitosis, Trends Cell Biol. 26 (2016) 766–775.

[8] E. Giarnieri, G.P. De Francesco, E. Carico, G. Midiri, C. Amanti, L. Giacomelli, et al., Giovagnoli, Alpha- and beta-tubulin expression in rectal cancer development, Anticancer Res. 25 (2005) 3237–3241.

[9] Y. Kouzu, K. Uzawa, H. Koike, K. Saito, D. Nakashima, M. Higo, et al., Overexpression of stathmin in oral squamous-cell carcinoma: correlation with tumour progression and poor prognosis, Br. J. Canc. 94 (2006) 717–723.

[10] S. Suzuki, T. Yokobori, B. Altan, K. Hara, D. Ozawa, N. Tanaka, et al., High stathmin 1 expression is associated with poor prognosis and chemoradiation resistance in esophageal squamous cell carcinoma, Int. J. Oncol. (2017).

[11] F. Wang, L.X. Wang, S.L. Li, K. Li, W. He, H.T. Liu, et al., Downregulation of stathmin is involved in malignant phenotype reversion and cell apoptosis in esophageal squamous cell carcinoma, J. Surg. Oncol. 103 (2011) 704–715.

[12] X. Zhang, J. Ji, Y. Yang, J. Zhang, L. Shen, Stathmin1 increases radioresistance by enhancing autophagy in non-small-cell lung cancer cells, OncoTargets Ther. 9 (2016) 2565–2574.

[13] H. Liu, A.J. Smith, S.S. Ball, Y. Bao, R.P. Bowater, N. Wang, et al., Sulforaphane promotes ER stress, autophagy, and cell death: implications for cataract surgery, J. Mol. Med. (Berl.) 95 (2017) 553–564.

[14] T. Wang, Q. Wang, R. Song, Y. Zhang, J. Yang, Y. Wang, et al., Cadmium induced inhibition of autophagy is associated with microtubule disruption and mitochondrial dysfunction in primary rat cerebral cortical neurons, Neurotoxicol. Teratol. 53 (2016) 11–18.

[15] P. Naumann, F. Fortunato, H. Zentgraf, M.W. Buchler, I. Herr, J. Werner, Autophagy and cell death signaling following dietary sulforaphane act independently of each other and require oxidative stress in pancreatic cancer, Int. J. Oncol. 39 (2011) 101–109.

[16] M.K. Singh, B. Sharma, P.K. Tiwari, The small heat shock protein Hsp27: present understanding and future prospects, J. Therm. Biol. 69 (2017) 149–154.

[17] N. Gan, Y.C. Wu, M. Brunet, C. Garrido, F.L. Chung, C. Dai, et al., Sulforaphane activates heat shock response and enhances proteasome activity through up-regulation of Hsp27, J. Biol. Chem. 285 (2010) 35528–35536.

[18] X. Ding, H. Li, H. Xie, Y. Huang, Y. Hou, Y. Yin, et al., A novel method to assay molecular chaperone activity of HSP70: evaluation of drug resistance in cancer treatment, Biosens. Bioelectron. 47 (2013) 75–79.

[19] Y. Xin, F. Yin, S. Qi, L. Shen, Y. Xu, L. Luo, et al., Parthenolide reverses doxorubicin resistance in human lung carcinoma A549 cells by attenuating NF-kappaB activation and HSP70 up-regulation, Toxicol. Lett. 221 (2013) 73–82.

[20] Y.H. Park, J.H. Seo, J.H. Park, H.S. Lee, K.W. Kim, Hsp70 acetylation prevents caspase-dependent/independent apoptosis and autophagic cell death in cancer cells, Int. J. Oncol. 51 (2017) 573–578.

[21] S. Kumar, J. Stokes 3rd, U.P. Singh, K. Scissum Gunn, A. Acharya, U. Manne, et al., Targeting Hsp70: a possible therapy for cancer, Canc. Lett. 374 (2016) 156–166.

[22] A.R. Goloudina, O.N. Demidov, C. Garrido, Inhibition of HSP70: a challenging anti-cancer strategy, Canc. Lett. 325 (2012) 117–124.

[23] M.Y. Sherman, V.L. Gabai, Hsp70 in cancer: back to the future, Oncogene 34 (2015) 4153–4161.

[24] D. Kumar, S. Shankar, R.K. Srivastava, Rottlerin-induced autophagy leads to the apoptosis in breast cancer stem cells: molecular mechanisms, Mol. Canc. 12 (2013) 171.
[25] Y.M. Kulkarni, V. Kaushik, N. Azad, C. Wright, Y. Rojanasakul, G. O'Doherty, et al., Autophagy-induced apoptosis in lung cancer cells by a novel digitoxin analog, J. Cell. Physiol. 231 (2016) 817–828.
[26] Y. An, W. Liu, P. Xue, Y. Zhang, Q. Wang, Y. Jin, Increased autophagy is required to protect periodontal ligament stem cells from apoptosis in inflammatory microenvironment, J. Clin. Periodontol. 43 (2016) 618–625.
[27] W.R. Pan, P.W. Chen, Y.L. Chen, H.C. Hsu, C.C. Lin, W.J. Chen, Bovine lactoferricin B induces apoptosis of human gastric cancer cell line AGS by inhibition of autophagy at a late stage, J. Dairy Sci. 96 (2013) 7511–7520.
[28] D.A. Gewirtz, The four faces of autophagy: implications for cancer therapy, Canc. Res. 74 (2014) 647–651.
[29] M. Rohde, M. Daugaard, M.H. Jensen, K. Helin, J. Nylandsted, M. Jaattela, Members of the heat-shock protein 70 family promote cancer cell growth by distinct mechanisms, Genes Dev. 19 (2005) 570–582.
[30] K. Lin, R. Yang, Z. Zheng, Y. Zhou, Y. Geng, Y. Hu, et al., Sulforaphane-cysteine-induced apoptosis via phosphorylated ERK1/2-mediated maspin pathway in human non-small cell lung cancer cells, Cell Death Dis. 3 (2017) 17025.
[31] H. Tian, Y. Zhou, G. Yang, Y. Geng, S. Wu, Y. Hu, et al., Sulforaphane-cysteine suppresses invasion via downregulation of galectin-1 in human prostate cancer DU145 and PC3 cells, Oncol. Rep. 36 (2016) 1361–1368.
[32] S. Wu, Y. Zhou, G. Yang, H. Tian, Y. Geng, Y. Hu, et al., Sulforaphane-cysteine induces apoptosis by sustained activation of ERK1/2 and caspase 3 in human glioblastoma U373MG and U87MG cells, Oncol. Rep. 37 (2017) 2829–2838.
[33] J.V. Cross, J.M. Rady, F.W. Foss, C.E. Lyons, T.L. Macdonald, D.J. Templeton, Nutrient isothiocyanates covalently modify and inhibit the inflammatory cytokine macrophage migration inhibitory factor (MIF), Biochem. J. 423 (2009) 315–321.
[34] L. Mi, Z. Xiao, B.L. Hood, S. Dakshanamurthy, X. Wang, S. Govind, et al., Covalent binding to tubulin by isothiocyanates. A mechanism of cell growth arrest and apoptosis, J. Biol. Chem. 283 (2008) 22136–22146.
[35] Z. Xiao, L. Mi, F.L. Chung, T.D. Veenstra, Proteomic analysis of covalent modifications of tubulins by isothiocyanates, J. Nutr. 142 (2012), 1377S-1381S.
[36] L. Mi, N. Gan, F.L. Chung, Aggresome-like structure induced by isothiocyanates is novel proteasome-dependent degradation machinery, Biochem. Biophys. Res. Commun. 388 (2009) 456–462.
[37] L. Mi, N. Gan, A. Cheema, S. Dakshanamurthy, X. Wang, D.C. Yang, et al., Cancer preventive isothiocyanates induce selective degradation of cellular alpha- and beta-tubulins by proteasomes, J. Biol. Chem. 284 (2009) 17039–17051.
[38] J. Lovric, S. Dammeier, A. Kieser, H. Mischak, W. Kolch, Activated raf induces the hyperphosphorylation of stathmin and the reorganization of the microtubule network, J. Biol. Chem. 273 (1998) 22848–22855.
[39] J.Y. Hu, Z.G. Chu, J. Han, Y.M. Dang, H. Yan, Q. Zhang, et al., The p38/MAPK pathway regulates microtubule polymerization through phosphorylation of MAP4 and Op18 in hypoxic cells, Cell. Mol. Life Sci. 67 (2010) 321–333.
[40] M. Kirschner, T. Mitchison, Beyond self-assembly: from microtubules to morphogenesis, Cell 45 (1986) 329–342.
[41] J.L. Webb, B. Ravikumar, D.C. Rubinsztein, Microtubule disruption inhibits autophagosome-lysosome fusion: implications for studying the roles of aggresomes in polyglutamine diseases, Int. J. Biochem. Cell Biol. 36 (2004) 2541–2550.
[42] A. Herman-Antosiewicz, D.E. Johnson, S.V. Singh, Sulforaphane causes autophagy to inhibit release of cytochrome C and apoptosis in human prostate cancer cells, Canc. Res. 66 (2006) 5828–5835.
[43] T.N. Nguyen, B.S. Padman, J. Usher, V. Oorschot, G. Ramm, M. Lazarou, Atg8 family LC3/GABARAP proteins are crucial for autophagosome-lysosome fusion but not autophagosome formation during PINK1/Parkin mitophagy and starvation, J. Cell Biol. 215 (2016) 857–874.
[44] C.H. Choi, Y.K. Jung, S.H. Oh, Autophagy induction by capsaicin in malignant human breast cells is modulated by p38 and extracellular signal-regulated mitogen-activated protein kinases and retards cell death by suppressing endoplasmic reticulum stress-mediated apoptosis, Mol. Pharmacol. 78 (2010) 114–125.
[45] H. Zhu, T. Yoshimoto, T. Yamashima, Heat shock protein 70.1 (Hsp70.1) affects neuronal cell fate by regulating lysosomal acid sphingomyelinase, J. Biol. Chem. 289 (2014) 27432–27443.
[46] J.I. Leu, J. Pimkina, A. Frank, M.E. Murphy, D.L. George, A small molecule inhibitor of inducible heat shock protein 70, Mol. Cell 36 (2009) 15–27.
[47] L.B. Frankel, J. Wen, M. Lees, M. Hoyer-Hansen, T. Farkas, A. Krogh, et al., MicroRNA-101 is a potent inhibitor of autophagy, EMBO J. 30 (2011) 4628–4641.
[48] X. Wang, M. Chen, J. Zhou, X. Zhang, HSP27, 70 and 90, anti-apoptotic proteins, in clinical cancer therapy (Review), Int. J. Oncol. 45 (2014) 18–30.
[49] W. Liu, Y. Chen, G. Lu, L. Sun, J. Si, Down-regulation of HSP70 sensitizes gastric epithelial cells to apoptosis and growth retardation triggered by H. pylori, BMC Gastroenterol. 11 (2011) 146.